Tetrahedron 68 (2012) 4368–4373

Contents lists available at SciVerse ScienceDirect

Tetrahedron

journal homepage: www.elsevier.com/locate/tet

Evaporation-induced self-assembly of *trans*-2-aminocyclopentanecarboxylic acid hexamers

Sunbum Kwon, Kyungtae Kang, Aram Jeon, Ji Hun Park, Insung S. Choi *, Hee-Seung Lee *

Molecular-Level Interface Research Center, Department of Chemistry, KAIST, Daejeon 305-701, Republic of Korea

ARTICLE INFO

Article history:
Received 10 October 2011
Received in revised form 25 January 2012
Accepted 24 February 2012
Available online 3 March 2012

Keywords:
Foldamer
β-Peptide
Self-assembly
Nanostructure

ABSTRACT

In this paper, we report the self-assembly phenomenon of *trans*-2-aminocyclopentanecarboxylic acid hexamer ($ACPC_6$) by the evaporation-induced self-assembly. The SEM and TEM analyses of the self-assembled 3D molecular architecture revealed the characteristic shape of hollow parallelepiped and its supramolecular chiral expression on surface. A systematic study with the derivatives of $ACPC_6$ showed the effect of the terminal groups of $ACPC_6$ on the particular 3D shape formation. We also found that water molecules played a crucial role in the formation of hollow morphogenesis under the evaporation-induced self-assembly condition, and a plausible formation mechanism was suggested.

1. Introduction

β-Peptide foldamers are oligomers of β-amino acids, and are known to adopt protein-like secondary structures, such as helices, strands, and turns.[1] Owing to their rigid and predictable conformational features in an aqueous solution, β-peptides have been used as excellent surrogates of natural peptides in many studies for biological applications.[2] The next challenge in this research field is to construct larger and sophisticated functional molecular systems that can mimic tertiary structures of proteins.[3] Thus, the increasing efforts have been devoted to understanding the self-assembly behavior of β-peptide foldamers. We and others have shown that helical β-peptide units agglomerate into highly organized supramolecular assemblies, the sizes of which are ranging from nano-sized oligomeric bundles to micro-sized architectures, by the precisely controlled noncovalent interactions.[4–7]

Previously we reported for the first time that a helical β-peptide heptamer composed of *trans*-(*S*,*S*)-2-aminocyclopentanecarboxylic acid residues ($ACPC_7$) self-assembled in an aqueous solution to form unprecedented three-dimensional (3D) molecular architectures that resembled the shapes of windmill, petal, and square-rod.[7a] More recently, we also found that the self-assembly of β-peptide hexamer ($ACPC_6$) gave rise to an intriguing molar-tooth shape.[7b] The rigid and unique conformational features of the 12-helical β-peptide building blocks in solution made it possible to generate the unusual 3D shapes that had never been obtained from any other organic molecular building blocks including conventional peptides.[8] A distinct advantage of β-peptides over α-peptides in self-assembly study is that one can easily make a relationship between the self-assembling components with predictable secondary structures and the observable 3D shapes. In other words, the effect of variations in the molecular structures of β-peptides could be immediately tractable at the morphologies of the resulting self-assembled entities, by which the governing parameters of self-assembly process should be controllable.

In the course of the previous self-assembly studies in an aqueous solution, we have been subjected to constant questioning as to which parameter of the self-assembly conditions plays a major role in determining the unusual and unique 3D morphological aspects. In particular, we are interested in the origin of non-spherical shape formation as well as the effect of the helical handedness of the building block on the self-assembled structures. In order to address this issue, we performed the self-assembly of $ACPC_6$ in a completely different experimental condition, which is the evaporation-induced self-assembly on surface. We reasoned that, if the unique 12-helical secondary structure of $ACPC_6$ is the major contributor of the 3D shape formation, the basic shapes from an identical building block should be similar or closely related to each other irrespective of the experimental conditions. Whereas the hydrophobic $ACPC_6$ molecules spontaneously self-assemble in an aqueous solution to reduce their hydrophobic surface areas when exposed to the solvophobic environment, the evaporation-induced self-assembly is driven by the progressive increase in the concentration of $ACPC_6$ upon solvent evaporation. Herein we report a 3D molecular architecture with a shape of hollow parallelepiped by the evaporation-induced

* Corresponding authors. E-mail address: hee-seung_lee@kaist.ac.kr (H.-S. Lee).

0040-4020/$ – see front matter © 2012 Elsevier Ltd. All rights reserved.
doi:10.1016/j.tet.2012.02.061

self-assembly of $ACPC_6$ on surface. The systematic variation in the molecular structure of $ACPC_6$ revealed that the size of the terminal groups played an important role in the 3D shaping of the architecture.

2. Results and discussion

2.1. Evaporation-induced self-assembly on surface

As building blocks for the assembly study, we prepared a pair of helical β-peptide hexamers ((*S*,*S*)-$ACPC_6$ and (*R*,*R*)-$ACPC_6$) that were exclusively composed of *trans*-(*S*,*S*)- and *trans*-(*R*,*R*)-2-aminocyclopentanecarboxylic acid residues, respectively (Fig. 1a). The N-terminal amino and C-terminal carboxylic acid groups were protected as *tert*-butyloxycarbonyl (Boc) carbamate and benzyl (Bn) ester, respectively.[8]

obtained from the identical building block in solution process, and the homogeneities in shape and size (ca. 5–10 μm) were not as good as those in solution.[7b]

The hollowness of the structure, in which two hollow basal faces are sharing an edge (Fig. 1d), is distinct from typical tubular shapes, in which two hollow basal faces are facing each other. The transmission electron microscopy (TEM) image showed clearly that the parallelepiped was divided into two rooms by a diagonal wall inside (Fig. 1f). Another interesting point is that the hollow interior showed a stair-like layered structure (Fig. 1e), which seemed to be related with stepwise growth mechanism. This type of unique structure has not been achievable via self-assembly of other organic molecules.

The evaporation-induced self-assembly study with the opposite enantiomer, (*R*,*R*)-$ACPC_6$, showed very interesting morphological phenomenon as shown in Fig. 2. The parallelepiped structures from

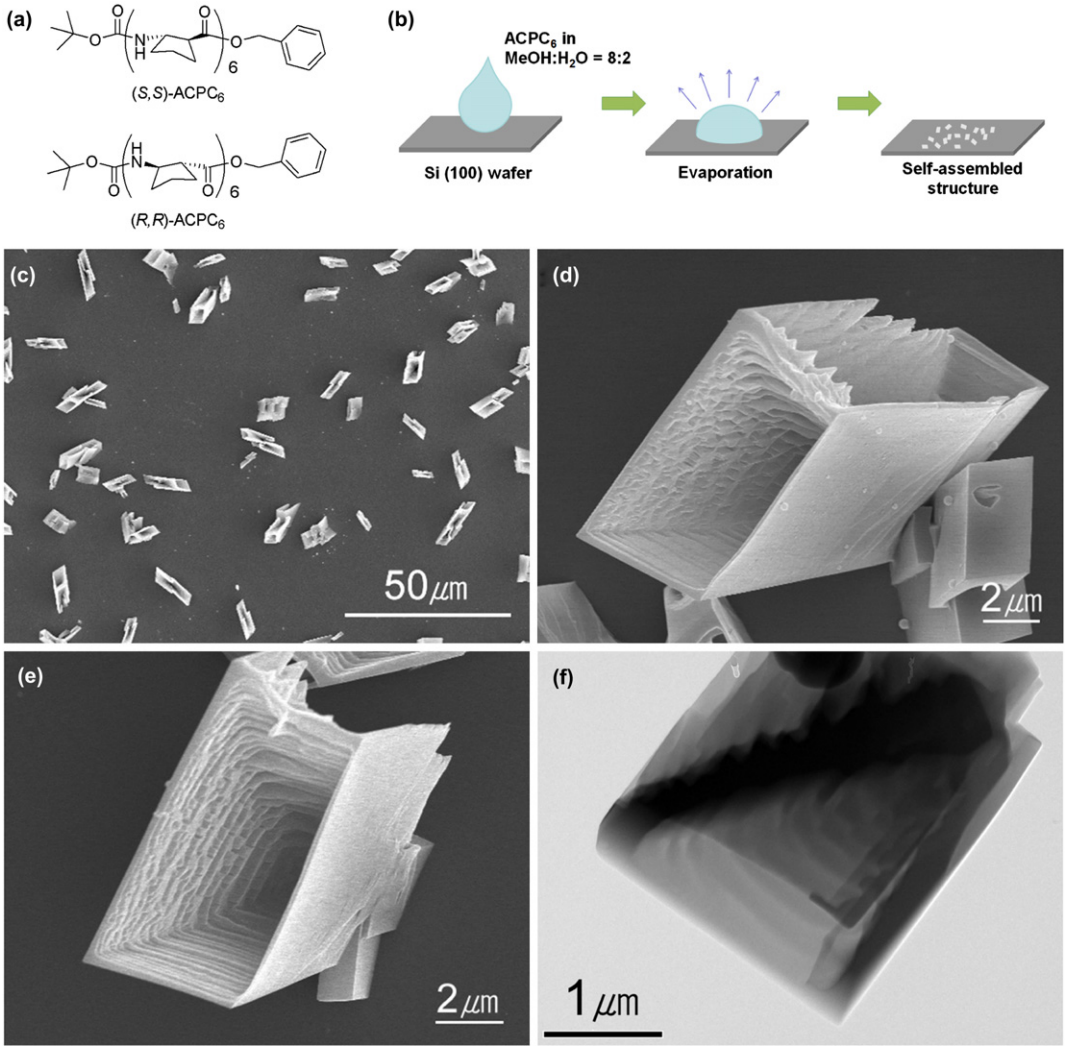

Fig. 1. a) Chemical structure of *trans*-(*S*,*S*)-ACPC hexamer ((*S*,*S*)-$ACPC_6$) and *trans*-(*R*,*R*)-ACPC hexamer ((*R*,*R*)-$ACPC_6$). b) Schematic representation of the evaporation-induced self-assembly process on surface. c–e) SEM images of self-assembled structures of $ACPC_6$ with a shape of hollow parallelepiped, f) TEM image of the parallelepiped indicating hollow interior.

The (*S*,*S*)-$ACPC_6$ was dissolved in methanol/water binary solvent mixture (1 mg mL^{-1}, methanol/water=8:2). An aliquot (3 μL) of the solution was dropped on Si (100) substrate, and then dried at 25 °C (Fig. 1b). After evaporation of solvents, white solids were formed on the surface. Scanning electron microscopy (SEM) analysis revealed very unusual self-assembled structure (Fig. 1c–e). The parallelepiped shape was completely different from the molar-tooth shape

the left-handed (*R*,*R*)-$ACPC_6$ are not superposable onto the shapes obtained from the right-handed (*S*,*S*)-$ACPC_6$ as if they were mirror images (Fig. 2a,b). This is not the case in our previous studies of self-assembly in solution, in which both self-assembling units resulted in almost identical 3D shape.[7b] The CD analyses in solution (Fig. 2c, 2.3 mM in methanol) and the solid state (Fig. 2, 0.65 wt % KBr pellet) clearly indicated that the inversion of the helical handedness of

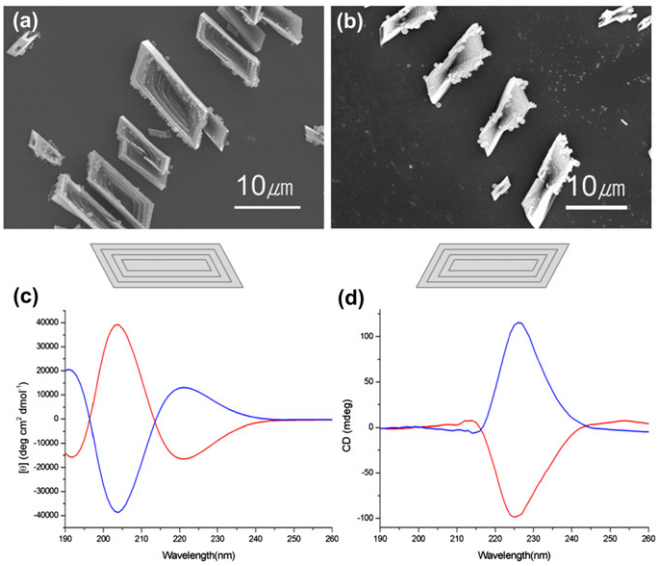

Fig. 2. a, b) SEM images along with 2D schematic illustration of the parallelepiped obtained from (*S*,*S*)-ACPC$_6$ and (*R*,*R*)-ACPC$_6$, respectively. c) Solution CD profiles (2.3 mM in methanol) of (*S*,*S*)-ACPC$_6$ (blue) and (*R*,*R*)-ACPC$_6$ (red), and d) Solid state CD spectra (0.65 wt % KBr pellet) of (*S*,*S*)-ACPC$_6$ (blue) and (*R*,*R*)-ACPC$_6$ parallelopiped (red).

ACPC$_6$ corresponds to the morphological inversion of the aggregates. The self-assembled powder of (*R*,*R*)-ACPC$_6$ showed the inverse CD signal of (*S*,*S*)-ACPC$_6$, although the minimum at 220 nm was slightly shifted to 225 nm, and the signals were not observable below 215 nm in the solid state CD experiment.

The chiral expression at the supramolecular level in the current study seemed to be attributed to the forced spatial restriction at the initial nucleation stage by the evaporation-induced self-assembly process, in which ACPC$_6$ molecules should be under the spatially nonequivalent environment. Thus, the self-assembly of the molecules in preferential direction arose to form the chiral morphogenesis.[9]

Interestingly, the thermogravimetric analysis (TGA) profile of the collected powder of the hollow parallelepiped showed 1.5% of weight loss during the heating process up to 100 °C (Fig. 3a, red line), and the differential scanning calorimetry (DSC) experiment clearly showed the endothermic reaction at 100 °C (Fig. 3a, green line). We interpreted the data from the thermal experiments as the inclusion of water molecules in the hollow self-assembled structure. This kind of solvation phenomena in crystal structure is commonly called pseudopolymorphism.[10] In the self-assembly process, water molecules participated actively in the crystal growing to be captured inside the structure. The as-prepared ACPC$_6$ did not show any evident thermal reaction in DSC experiment (data not shown). The hydration in the hollow parallelepiped was also supported by the different powder X-ray diffraction (PXRD) patterns of the parallelepiped from those of the as-prepared ACPC$_6$ (Fig. 3b). Notably, the PXRD patterns of the hollow parallelepiped were also different from that of the self-assembled structure of ACPC$_6$ in solution process.[7b] These results implied that a different self-assembly method could result in the 3D shape alteration of the self-assembled structure along with the change of crystallinity.

2.2. Self-assembly of ACPC$_6$ analogues

To investigate the relationship between the molecular structure of building block and the self-assembled structure, we synthesized a series of ACPC$_6$ analogues with different end groups (**1**–**4** in Fig. 4) and monitored the self-assembled structures from the evaporation-induced self-assembly by SEM. [11] None of the analogues provided

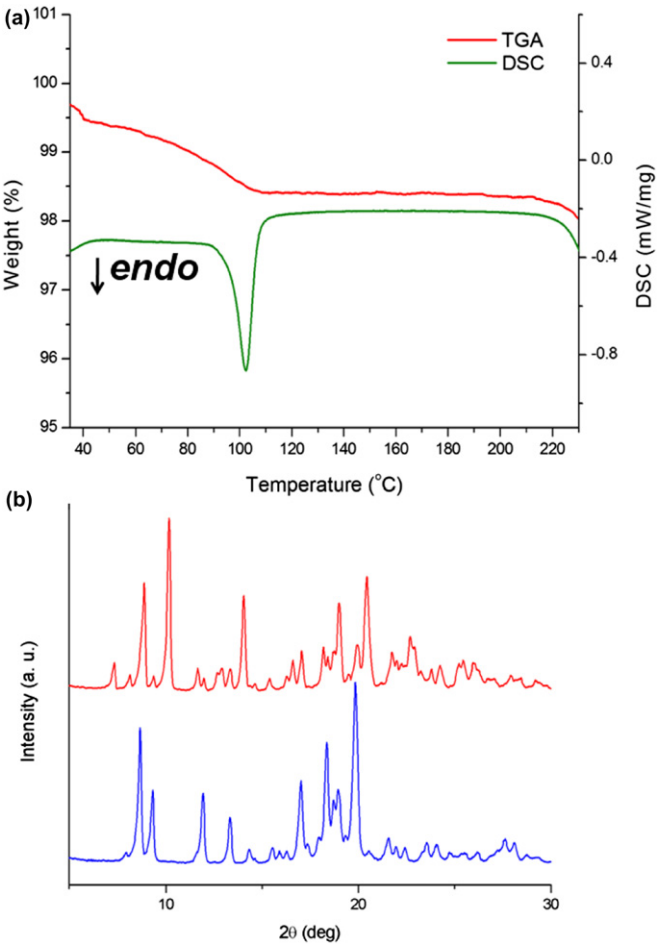

Fig. 3. a) DSC-TGA profile of the hollow parallelepiped. b) PXRD patterns of the hollow parallelepiped (red) and the as-prepared ACPC$_6$ (blue).

the hollow parallelepiped, suggesting that both Boc and benzyl groups are necessary for inducing the unique 3D shape formation. When the N-terminal Boc group remained intact and the C-terminal benzyl group was eliminated, the self-assembled structure of **1** became 2D parallelogrammatic plates (Fig. 4a), suggesting that the benzyl group played an important role in the molecular packing in the perpendicular direction of the plate. Interestingly, an asymmetrically grown dendritic plate was obtained if the smaller methyl group was introduced at the C-terminus instead of benzyl group (Fig. 4b). On the other hand, N-terminal acetyl-protected benzyl ester **3** self-assembled into micro-sized belts (Fig. 4c), and its carboxylic acid version **4** showed round disks (Fig. 4d).

The experimental results provided an insight into the relationship between molecular structure and its assembly shape, from which we are able to control the self-assembly process. First of all, a necessary and sufficient criterion for 3D shape formation is the existence of bulky groups, such as Boc and benzyl, at both termini of ACPC$_6$. As long as Boc group remains at the N-terminus intact (**1** and **2**), one can keep away from the situations of predominant unidirectional growth or spherical shape formation.

2.3. A proposed mechanism

To investigate how the characteristic hollow morphogenesis occurs, we monitored the self-assembled structures of (*S*,*S*)-ACPC$_6$ upon variation in the methanol/water ratio of the binary solvent system. When pure methanol was used instead of methanol/water mixture, a similar shape of parallelepiped was obtained. However,

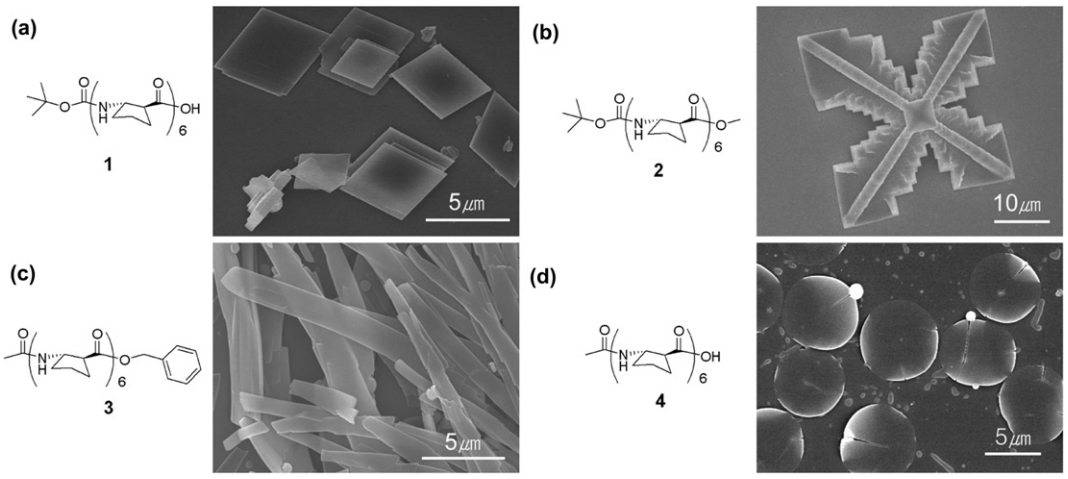

Fig. 4. Chemical structures and SEM images of the self-assembled structures of a) BocNH-ACPC$_6$-OH, b) BocNH-ACPC$_6$-OMe, c) AcNH-ACPC$_6$-OBn, and d) AcNH-ACPC$_6$-OH obtained from the evaporation-induced self-assembly method.

the structure was not hollow (Fig. 5a) but instead patterned with multiple parallelogrammatic steps on the face, which resembled the layered interior of the hollow parallelepiped (Fig. 5b). This observation provided us a thought that water might play a crucial role in generating the hollow structure. To confirm this idea, we performed the self-assembly in the solvents of various water content. As expected, the gradual increase of water content in binary solvent mixture induced bigger cavity on the face of the parallelepiped (Fig. 5c–e).

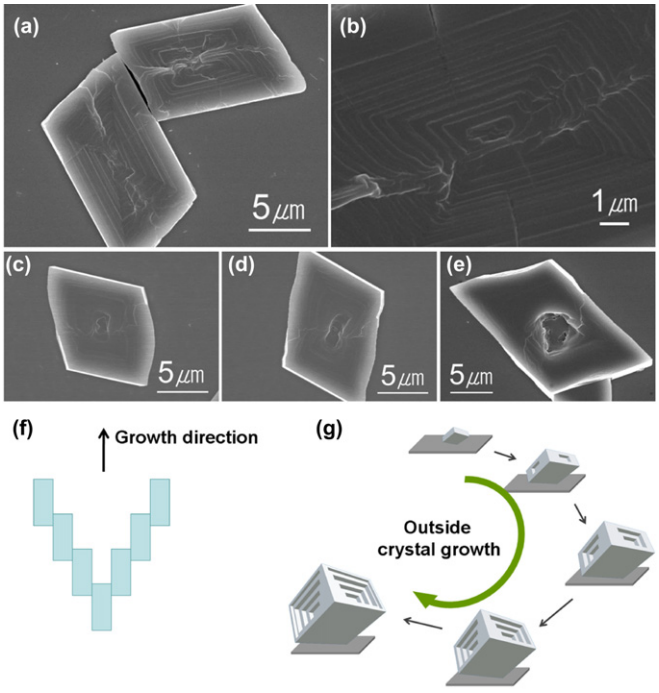

Fig. 5. a) SEM image of the self-assembled structure of the parallelepiped obtained from methanol solution, and b) its magnified view. c-e) SEM images of the parallelepiped obtained from methanol/water binary solvents with increasing water proportion (0.1, 1, and 5%), respectively. f) Schematic illustration of skeletal crystal growth (reproduced from Iwanaga, 1974). g) Proposed mechanism of hollow parallelepiped formation.

Based on the experimental observations and the following established researches, we propose a mechanism of hollow parallelepiped formation by the evaporation-induced self-assembly of ACPC$_6$ as an analogous process of diffusion-limited crystallization. Several studies have demonstrated that, under diffusion-limited condition, the speed of crystal growth at the edge is more rapid than that at the inner side.[12,13] In many cases found in inorganic crystals, they lose the polyhedral shape stability above high supersaturation, and evolve into hollow or tubular structures. At still higher supersaturation, crystal growth rate increases and thus skeletal or dendritic structures occur. This is well-explained by Iwanaga's model,[14] in which consecutive nucleation on growing crystal faces leads to the increase in diameter of hollowness and the stair-like self-assembled morphology (Fig. 5f).[15] In this study, at the initial stage of evaporation-induced self-assembly process, the proportion of water (poor solvent) in methanol/water mixture gradually increases due to the lower boiling point of methanol, and subsequently the concentration of ACPC$_6$ reaches to supersaturation. After the nuclei are generated, they grow into tiny parallelepiped crystal by diffusion-mediated mass transport. At this stage, new nucleation on the surfaces of the growing crystal occurs, and the initial crystal faces are covered by further-growing layer. This nucleation-growth repeating process produces the hollow parallelepiped with stair-like interior (Fig. 5g).

When the evaporation-induced self-assembly of ACPC$_6$ was performed on the patterned Au surface with alternating hydrophilic and hydrophobic areas, the hollow parallelepiped was formed exclusively on the hydrophobic area (Fig. 6a). The experimental result implied that the hydrophobic nature of ACPC$_6$ molecules was attracted by the hydrophobic surface, thus the initial nucleation preferentially occurred on the hydrophobic area. It was a supporting evidence of our proposed mechanism that the evaporation-induced self-assembly of β-peptide foldamer followed the analogous process of nucleation-based crystallization, ruling out the possibility of colloidal particle assembly by convective flow in droplet.

3. Conclusion

In summary, we have obtained very unique 3D molecular architectures with a shape of hollow parallelepiped by the evaporation-induced self-assembly of a 12-helical β-peptide hexamer. The helical handedness of self-assembling units could be well-expressed at the assembled structures in this experimental condition. The hollowness of the parallelepiped structure seemed to be attributed to the participation of water molecules in the assembly process. We also found that the relationship between the molecular structure and its resulting shape of assembly by the systematic self-assembly studies using structurally relevant molecules. Finally, a plausible self-assembly mechanism was proposed from the experimental data.

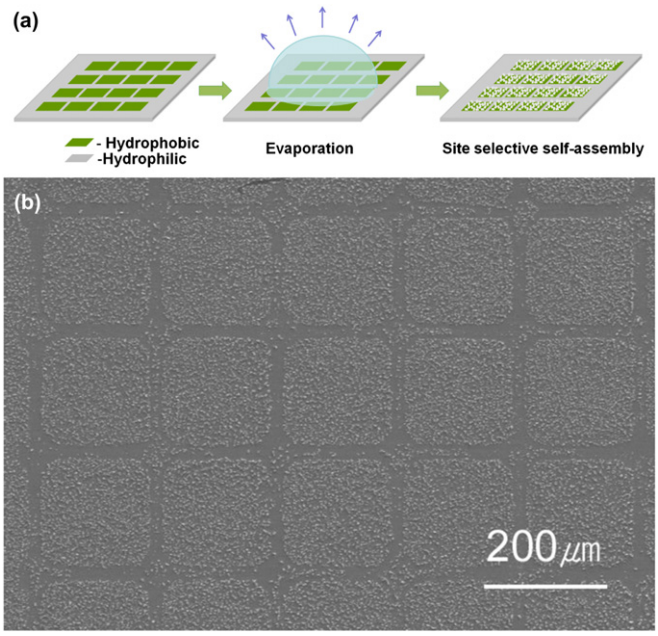

Fig. 6. a) Schematic representation of site-selective self-assembly process on Au surface with alternating hydrophobic and hydrophilic pattern. b) SEM image of self-assembled structures on the Au surface (border: hydrophilic, inside the squares: hydrophobic).

The self-assembly study of peptidic or nonpeptidic foldamers is still in its infancy, but the knowledge from the self-assembly of various structures of foldamers will provide very useful design principles toward the construction of functional assemblies and find many potential applications, such as catalysis, optical sensors and lithographic templates in the near future.[16–18]

4. Experimental section

4.1. General methods

All chemicals for the preparation of the $ACPC_6$ were purchased from Sigma-Aldrich, Acros, Junsei, and TCI, and were used without further purification. High purity water was generated by a Milli-Q apparatus (Millipore). For the evaporation-induced self-assembly experiment, each self-assembling component was dissolved in methanol (1 mg mL^{-1}) or binary solvent mixture (1 mg mL^{-1}, methanol/water=8:2). An aliquot (3 μL) of the solution was dropped on Si (100) substrate and then dried under ambient condition (1 atm, 25 °C) for further analysis.

Scanning electron microscopy images were obtained using a field-emission scanning electron microscope (FE-SEM, Hitachi S-4800, Japan) at an acceleration voltage of 10 kV after Pt-coating (SCD 050 platinum evaporator, Bal-tec, Germany). Transmission electron microscopy images were obtained using a field-emission scanning electron microscope (FE-TEM, Tecnai G2 F30, Philips). Thermogravimetry analysis and differential scanning calorimetry were performed using TG 209 F3 and DSC 204 F1, respectively, with increasing temperature of 10 °C/min under N_2 (NETZSCH, Germany). Powder X-ray diffraction patterns were obtained from a multi-purpose attachment X-ray diffractometer (Rigaku, D/Max-2500) equipped with a pyrolytic graphite (002) monochromator. Characteristic Cu Kα radiation was used as an incident beam (λ=1.54178 Å), and the diffraction patterns were scanned over 2θ values ranging from 2° to 70° in increments of 0.02° at room temperature. Circular dichroism spectra were obtained by Jasco-815 spectrometer (Jasco. Inc., Japan) with methanolic solution of $ACPC_6$ (2.3 mM), and sample cell of path length 1 mm was used. Solid state CD experiments were performed with 0.65 wt% of $ACPC_6$ microcrystalline KBr pellets (1 mm thickness).

4.2. Preparation of patterned Au surface

For the preparation of hydrophilic/hydrophobic patterned Au surface, poly(dimethylsiloxane) (PDMS) was used as a stamping material. PDMS stamps were prepared as reported previously.[19] In short, a negative photoresist (SU8-50, Microchem) was spin-coated onto a cleaned silicon wafer. Patterns were then generated by photolithography and subsequently developed on the wafer. The patterned wafer, 'master', was then silanized with (tridecafluoro-1,1,2,2,-tetrahydrooctyl)trichlorosilane under vacuum for 2 h. This step enabled the master to be easily separated from the cured PDMS stamps. For the PDMS stamps, a 1:10 (v/v) mixture of Sylgard 184 silicon elastomer curing agent (Dow Corning) and Sylgard 184 silicon elastomer base (Dow Corning) was cast, cured for 6 h at 60 °C, and carefully peeled off from the master. The PDMS stamp was wetted by spin-coating with an ethanolic solution of 16-mercaptohexadecanoic acid (1 mM) and stamped to the Au surface for generating hydrophilic regions. The remaining region of Au surface was subsequently tailored to be hydrophobic by immersing the substrate to an ethanolic solution of 16-mercaptohexadecane (1 mM) for 3 h.

4.3. BocNH-$ACPC_6$-OH (compound 1)

$ACPC_6$ (350 mg, 0.4 mmol) was dissolved in ethanol (20 mL), and 10% Pd on activated charcoal (10 mg) was added. Under the H_2 atmosphere, the reaction mixture was stirred until the starting material was consumed. After the reaction was finished, the solution was filtered through Celite pad. White solid was obtained after solvent evaporation under reduced pressure and used without further purification (310 mg, 99%). ^{1}H NMR (pyridine-d_5, 400 Hz) δ 9.40 (t, J=5.4 Hz, 2H, NH), δ 9.12 (d, J=9.1 Hz, 1H, NH), δ 8.87 (d, J=8.5 Hz, 1H, NH), δ 8.47 (d, J=9.3 Hz, 1H, NH), δ 8.37 (d, J=8.3 Hz, 1H, NH), δ 4.87 (quintet, J=7.7 Hz, 1H, CONHC*H*), δ 4.78–4.6 (m, 4H, CONHC*H*), δ 4.48 (quintet, J=7.9 Hz, 1H, CONHC*H*), δ 3.88 (quintet, J=5.3 Hz, 1H, NHCOC*H*), δ 3.04 (q, J=8.5 Hz, 1H, NHCOC*H*), δ 2.89 (sextet, J=7.8 Hz, 2H, NHCOC*H*), δ 2.74 (q, J=8.6 Hz, 1H, NHCOC*H*), δ 2.62 (q, J=7.4 Hz, 1H, NHCOC*H*), δ 2.43–1.68 (m, 36H), δ 1.51 (s, 9H, CH_3). MS calcd for $C_{41}H_{64}N_6O_9$: 784.4735; found (MALDI-TOF), 785.65 $[M+H]^+$, 807.97 $[M+Na]^+$.

4.4. BocNH-$ACPC_6$-OMe (compound 2)

Cesium carbonate (100 mg, 0.31 mmol) and iodomethane (0.2 mL, 3.2 mmol) were added to a solution of compound **1** (200 mg, 0.255 mmol) in DMF (20 mL), and the resulting mixture was stirred for 3 h at room temperature. After the reaction was complete, DMF was removed under reduced pressure. The resulting residue was dissolved in CH_2Cl_2, and washed with aqueous NH_4Cl solution, and then the organic layer was dried over $MgSO_4$. After the removal of solvent, the crude product was purified by column chromatography (MeOH/$CHCl_3$ 1:12). The oily product was precipited in a mixture of CH_2Cl_2 and heptane to form white solid (200 mg, 98%). ^{1}H NMR (pyridine-d_5, 400 Hz) δ 9.38 (d, J=8.2 Hz, 1H, NH), δ 9.03 (d, J=9.1 Hz, 1H, NH), δ 8.91 (d, J=7.8 Hz, 1H, NH), δ 8.80 (d, J=8.3 Hz, 1H, NH), δ 8.43 (d, J=9.3 Hz, 1H, NH), δ 8.35 (d, J=8.3 Hz, 1H, NH), δ 5.04 (quintet, J=7.4 Hz, 1H, CONHC*H*), δ 4.95–4.84 (m, 2H, CONHC*H*), δ 4.8–4.7 (m, 2H, CONHC*H*), δ 4.47 (quintet, J=7.8 Hz, 1H, CONHC*H*), δ 3.65 (s, 3H, CH_3), δ 3.50 (dt, J=9, 5.8 Hz, 1H, NHCOC*H*), δ 3.19 (dt, J=9, 5.8 Hz, 1H, NHCOC*H*), δ 2.95–2.88 (quintet, J=7.4 Hz, 2H, NHCOC*H*), δ 2.74 (q, J=8 Hz, 1H, NHCOC*H*), δ 2.62 (q, J=7.2 Hz, 1H, NHCOC*H*), δ 2.56–1.6 (m, 36H),

δ 1.51 (s, 9H, CH_3). MS calcd for $C_{42}H_{66}N_6O_9$: 798.4891; found (MALDI-TOF), 800.08 $[M+H]^+$, 822.03 $[M+Na]^+$.

4.5. AcNH-ACPC$_6$-OBn (compound 3)

HCl (4 N) in dioxane (5 mL) was added to $ACPC_6$ (180 mg, 0.21 mmol) under N_2, and the solution was stirred for 1 h. After the deprotection of Boc group, dioxane was removed by evaporation under reduced pressure. The resulting salt was dissolved in CH_2Cl_2, and then triethylamine (0.1 mL, 0.72 mmol) and acetic anhydride (0.1 mL, 1.06 mmol) were sequentially added to the solution. The reaction mixture was stirred for 3 h at room temperature, and quenched with aqueous NH_4Cl solution. The organic layer was dried over $MgSO_4$, and concentrated under reduced pressure. The resulting yellow oil was purified by column chromatography (MeOH/$CHCl_3$ 1:12). The product was precipitated in a mixture of CH_2Cl_2 and heptanes to give white solid (108 mg, 64.3%) ^{1}H NMR (pyridine-d_5, 400 Hz) δ 9.26 (d, J=8.6 Hz, 1H, NH), δ 9.03 (d, J=7.4 Hz, 1H, NH), δ 8.99–8.96 (m, *2*H, NH), δ 8.80 (d, J=8.8 Hz, 2H, NH), δ 7.50 (d, J=8.0 Hz, 2H, ArH), δ 7.32 (t, J=7.4 Hz, 2H, ArH), δ 7.24 (t, J=7.6 Hz, 1H, ArH), δ 5.37 (*A*B quartet, J=12.7 Hz, 1H, $ArCH_2$), δ 5.23 (A*B* quartet, J=12.7 Hz, 1H, $ArCH_2$), δ 5.07 (quintet, J=5.7 Hz, 1H, CONHC*H*), δ 4.90–4.84 (m, 2H, CONHC*H*), δ 4.82–4.64 (m, 3H, CONHC*H*), δ 3.60 (dt, J=8.8, 5.9 Hz, 1H, NHCOC*H*), δ 3.19 (dt, J=8.8, 6.3 Hz, 1H, NHCOC*H*), δ 2.96–2.89 (m, 2H, NHCOC*H*), δ 2.75–2.68 (m, 2H, NHCOC*H*), δ 2.49–1.6 (m, 39H), MS calcd for $C_{45}H_{64}N_6O_8$: 816.4786; found (MALDI-TOF), 818.33 $[M+H]^+$, 840.36 $[M+Na]^+$.

4.6. AcNH-ACPC$_6$-OH (compound 4)

Compound **3** (81 mg, 0.1 mmol) was dissolved in ethanol (10 mL), and 10% Pd on activated charcoal (5 mg) was added. Under H_2, the reaction mixture was stirred until the starting material was consumed. After the reaction was finished, the solution was filtered through Celite pad. White solid was obtained after solvent evaporation under reduced pressure and used without further purification (71 mg, 99%). ^{1}H NMR (pyridine-d_5, 400 Hz) δ 9.41 (d, J=6.5 Hz, 1H, NH), δ 9.31 (d, J=8.6 Hz, 1H, NH), δ 9.11–9.05 (m, *2*H, NH), δ 8.89–8.83 (m, 2H, NH), δ 4.89–4.64 (m, 6H, CONHC*H*), δ 3.84 (quintet, J=3.8 Hz, 1H, NHCOC*H*), δ 3.04 (q, J=7.8 Hz, 1H, NHCOC*H*), δ 2.93–2.89 (m, 2H, NHCOC*H*), δ 2.75 (q, J=8.6 Hz, 1H, NHCOC*H*), δ 2.73 (q, J=8.6 Hz, 1H, NHCOC*H*), δ 2.41–1.62 (m, 39H), MS calcd for $C_{38}H_{58}N_6O_8$: 726.4316; found (MALDI-TOF), 728.295 $[M+H]^+$, 750.292 $[M+Na]^+$.

Acknowledgements

This work was supported by a Basic Science Research Program of the National Research Foundation of Korea (NRF) grant funded by the Ministry of Education, Science and Technology (2009-0084449, 2011-0012141, and 2011-0001318).

References and notes

1. (a) Cheng, R. P.; Gellman, S. H.; DeGrado, W. F. *Chem. Rev.* **2001**, *101*, 3219–3232; (b) Seebach, D.; Beck, A. K.; Bierbaum, D. J. *Chem. Biodiversity* **2004**, *1*, 1111–1239; (c) Goodman, C. M.; Choi, S.; Shandler, S.; DeGrado, W. F. *Nat. Chem. Biol.* **2007**, *3*, 252–262; (d) Guichard, G.; Huc, I. *Chem. Commun.* **2011**, 5933–5941; (e) Hecht, S.; Huc, I. *Foldamers: Structure, Properties, and Applications*; Wiley-VCH: Weinheim, Germany, 2007.
2. (a) Porter, E. A.; Wang, X.; Lee, H. –S.; Weisblum, B.; Gellman, S. H. *Nature* **2000**, *404*, 565; (b) Müller, M. M.; Windsor, M. A.; Pomerantz, W. C.; Gellman, S. H.; Hilvert, D. *Angew. Chem., Int. Ed.* **2009**, *48*, 922–925; (c) Choi, S.; Isaacs, A.; Clements, D.; Liu, D.; Kim, H.; Scott, R. W.; Winkler, J. D.; DeGrado, W. F. *Proc. Natl. Acad. Sci. U.S.A.* **2009**, *106*, 6968–6973; (d) Lee, E. F.; Sadowsky, J. D.; Smith, B. J.; Czabotar, P. E.; Peterson-Kaufman, K. J.; Colman, P. M.; Gellman, S. H.; Fairlie, W. D. *Angew. Chem., Int. Ed.* **2009**, *48*, 4318–4322.
3. (a) Horne, W. S.; Price, J. L.; Keck, J. L.; Gellman, S. H. *J. Am. Chem. Soc.* **2007**, *129*, 4178–4180; (b) Daniels, D. S.; Petersson, E. J.; Qiu, J. X.; Schepartz, A. *J. Am. Chem. Soc.* **2007**, *129*, 1532–1533; (c) Martinek, T. A.; Mándity, I. M.; Fülöp, L.; Tóth, G. K.; Vass, E.; Hollósi, M.; Forró, E.; Fülöp, F. *J. Am. Chem. Soc.* **2006**, *128*, 13539–13544; (d) Delsuc, N.; Massip, S.; Léger, J. –M.; Kauffmann, B.; Huc, I. *J. Am. Chem. Soc.* **2011**, *133*, 3165–3172; (e) Ferrand, Y.; Kendhale, A. M.; Garric, J.; Kauffmann, B.; Huc, I. *Angew. Chem., Int. Ed.* **2010**, *49*, 1778–1781; (f) Tanaka, Y.; Katagiri, H.; Furusho, Y.; Yashima, E. *Angew. Chem., Int. Ed.* **2005**, *44*, 3867–3870.
4. Goodman, J. L.; Petersson, E. J.; Daniels, D. S.; Qiu, J. X.; Schepartz, A. *J. Am. Chem. Soc.* **2007**, *129*, 14746–14751.
5. (a) Pomerantz, W. C.; Yuwono, V. M.; Pizzey, C. L.; Hartgerink, J. D.; Abbott, N. L.; Gellman, S. H. *Angew. Chem., Int. Ed.* **2008**, *47*, 1241–1244; (b) Pomerantz, W. C.; Yuwono, V. M.; Drake, R.; Hartgerink, J. D.; Abbott, N. L.; Gellman, S. H. *J. Am. Chem. Soc.* **2011**, *133*, 13604–13613.
6. Martinek, T. A.; Hetényi, A.; Fülöp, L.; Mándity, I. M.; Tóth, G. K.; Dékány, I.; Fülöp, F. *Angew. Chem., Int. Ed.* **2006**, *45*, 2396–2400.
7. (a) Kwon, S.; Jeon, A.; Yoo, S. H.; Chung, I. S.; Lee, H.-S. *Angew. Chem., Int. Ed.* **2010**, *49*, 8232–8236; (b) Kwon, S.; Shin, H. S.; Gong, J.; Eom, J.-H.; Jeon, A.; Yoo, S. H.; Chung, I. S.; Cho, S. J.; Lee, H.-S. *J. Am. Chem. Soc.* **2011**, *133*, 17618–17621.
8. (a) Appella, D. H.; Christianson, L. A.; Klein, D. A.; Powell, D. R.; Huang, X.; Barchi, J. J.; Gellman, S. H. *Nature* **1997**, *387*, 381–384; (b) Appella, D. H.; Christianson, L. A.; Klein, D. A.; Richards, M. R.; Powell, D. R.; Gellman, S. H. *J. Am. Chem. Soc.* **1999**, *121*, 7574–7581.
9. The unique parallellopiped shape was obtained only when we used the enantiomerically pure monomer. The mixtures of (*S*,*S*)- and (*R*,*R*)-$ACPC_6$ (1:1, 1:3, or 3:1) did not provide well-defined 3D shapes but irregular-shaped aggregates.
10. Tedesco, C.; Erra, L.; Immediata, I.; Gaeta, C.; Brunelli, M.; Merlini, M.; Meneghini, C.; Pattison, P.; Neri, P. *Cryst. Growth Des.* **2010**, *10*, 1527–1533.
11. Reches, M.; Gazit, E. *Nat. Nanotechnol.* **2006**, *1*, 195–200.
12. Nanev, C. N. *Prog. Cryst. Growth Charact. Mater.* **1997**, *35*, 1–26.
13. Eddleston, M. D.; Jones, W. *Cryst. Growth Des.* **2010**, *10*, 365–370.
14. Iwanaga, H.; Shibata, N. *J. Cryst. Growth* **1974**, *24–25*, 357–361.
15. Hsieh, Y.-T.; Leong, T.-I.; Huang, C.-C.; Yeh, C.-S.; Sun, I.-W. *Chem. Commun.* **2010**, 484–486.
16. Juwarker, H.; Suk, J.-m.; Jeong, K.-S. *Chem. Soc. Rev.* **2009**, *38*, 3316–3325.
17. Zhang, X. X.; Bradshaw, J. S.; Izatt, R. M. *Chem. Rev.* **1997**, *97*, 3313–3361.
18. Han, T. H.; Ok, T.; Kim, J.; Shin, D. O.; Ihee, H.; Lee, H.-S.; Kim, S. O. *Small* **2010**, *6*, 945–951.
19. Lee, B. S.; Lee, J. K.; Kim, W. –J.; Jung, Y. H.; Sim, S. J.; Lee, J.; Choi, I. S. *Biomacromolecules* **2007**, *8*, 744–749.